

# Entropy–Enthalpy Compensations in Solutions of Dual Character Molecules with Polymeric Chromatographic Liquid Phases

Jan-Chan Huang\*

Plastics Engineering Department, University of Massachusetts Lowell, Lowell, Massachusetts 01854

Richard J. Sheehan and Stanley H. Langer

Department of Chemical and Biological Engineering, University of Wisconsin–Madison, Madison, Wisconsin 53706

Received: September 9, 2004; In Final Form: November 17, 2004

Careful gas chromatographic studies provide thermodynamic data for insights into solution processes in nonvolatile solvents. Using 24 solutes and five stationary phases, several entropy–enthalpy compensation effects in the thermodynamics of solution were identified. Despite solute structure differences, when excess enthalpy and entropy of solutions were examined, entropy–enthalpy compensation effects were found in solvents dominated by single types of interaction: squalane and, to some extent, methoxy poly(ethylene oxide) (PEO). The main reason for the absence of linearity in other solvents is pure solute state interactions in the reference state and the multicharacter nature of solvents. In this study, consideration of solute state interactions was removed through examination of the thermodynamics of transfer between solvent pairs. It was found that solute transfers from squalane to poly[methyl(trifluoropropyl)siloxane] (QF-1) and to poly-(methylphenyl) (DC-550) also gave linear relationships. The former system contains a second correlation for ester type solutes. The transfer data for squalane to poly(methylsiloxane) (DC-200) had smaller ranges and were more scattered. The effects of derivatizing groups on the transfer enthalpy and entropy were treated as a summation of hydrocarbon cores with the derivative groups. The group properties of transfer then also show entropy–enthalpy compensation effects. Many solution effects could be explained on the basis of solvent composition and local interactions with solutes.

## 1. Introduction

Gas–liquid chromatography (GLC) has been applied for many years for measuring solute vapor solubility in high molecular weight and polymeric materials<sup>1–4</sup> as well as for other physicochemical information.<sup>5–11</sup> Most physicochemical studies focused on solutes that were similar to the monomer or the structural units of polymers, such as alkanes, aromatics, oxygenated, or chlorinated compounds. These solute molecules generally have been relatively small, with single functional groups, belonging to homologous series. Their solution properties generally have been explained in terms of three common types of interactions: dispersion forces, dipoles, and hydrogen bonding. Fluorocarbons interact differently. Fluorinated compounds have received little attention despite their frequent application in derivatization for gas chromatographic analysis. In our earlier studies<sup>12,13</sup> of solution thermodynamic properties, several derivatives of hydroxylic compounds were used. These derivatives included acetates, trimethylsilyl ethers (TMSE), trifluoroacetates (TFA), and pentafluoropropionates (PFP), so-called “dual character” molecules,<sup>12,13</sup> which consist of two parts with dissimilar properties.

In many GLC studies the excess free energies of solution, measured at different temperatures, were separated into enthalpies and entropies of solution. Plots of entropy vs enthalpy were used in discussions of solution thermodynamics with GLC.<sup>10–16</sup> Linear relationships frequently were found and cited as entropy–

enthalpy compensation effects, extrathermodynamic phenomena, or isokinetic relationships. They were found for a variety of thermodynamic and kinetic processes.<sup>9–28</sup> Despite their utility, these relationships also have led to some misunderstanding and controversy. In essence, entropy–enthalpy compensation refers to the experimental observation of a linear relationship between enthalpy ( $\Delta H$ ) and entropy ( $\Delta S$ ) for related processes. The entropy–enthalpy compensation effect can be represented in the following form:

$$\Delta H = \beta \Delta S + \alpha \quad (1)$$

The parameter  $\beta$ , positive with temperature unit, is designated the “compensation” temperature. A positive  $\beta$  indicates that when there is a positive variation for a series of solutes, there is an increase in the entropy, which compensates for some of the change. The result is a smaller change in  $\Delta G$  relative to  $\Delta H$ . Experimental results of  $\Delta H$  and  $\Delta S$  obtained from free energies for a series of temperatures have been used frequently for the plots. However, Krug, Hunter, and Grieger<sup>24</sup> demonstrated that when enthalpy is calculated using the temperature dependence of free energies, propagated errors often give a straight line with a slope equal to the average temperature of the experimental measurements. Therefore, statistical errors tend to bias the extra-thermodynamic relationship unless the slope of the entropy–enthalpy plot happens to be different from the average of the experimental temperatures. Using a general statistical mechanical model, Sharp<sup>22</sup> showed that a correlation can occur with a slope within 20% of the experimental temperature. This behavior is insensitive to the model details,

\* Corresponding author. E-mail: Jan\_Huang@uml.edu. Tel: 978-934-3428. Fax: 978-458-4141.

thus revealing little extra-thermodynamic or causal information about the system.

Krug et al. suggested a simple way to minimize the influence of experimental errors.<sup>24</sup> From statistical considerations, they concluded that enthalpy-free energy plots are better criteria for evaluating extrathermodynamic relationships than entropy–enthalpy plots. A simple explanation originates from the free energy relationship,  $G = H - TS$ . Because  $H$  and  $S$  have different signs, for any given  $G$  an error in  $H$  tends to create a corresponding error in  $S$  values. In contrast, the signs of  $G$  and  $H$  are the same and they are on opposite sides of the equation, thus preventing the error from being incorporated into any correlation. Plots using free energies have an added advantage in that free energies in solution thermodynamic studies are linearly related to the logarithms of activity coefficients. It is these activity coefficients that are most pertinent to many separation processes.

Li and Carr<sup>26</sup> in their recent discussion of “entropy–enthalpy compensation” in gas chromatography noted that for many enthalpy-free energy plots only solutes belonging to homologous series produce linear free energy relationships. This observation is not unexpected because the solution thermodynamic properties represent the differences of properties between solute and solution states. In many instances, both solvents and solutes are multifunctional molecules. The functional groups may move or rotate to contact other functional groups to achieve a minimum energy state but the process may be compensated by an entropy change. The final state is determined by the difference in free energy. This leads to many possible combinations in solute liquids as well as solution states, and a simple linear relationship would not exist. There are two situations where one might expect an entropy–enthalpy compensation effect. One is in homologous series where enthalpy and entropy might be functions of solute chain length and are linear to each other. This has been discussed by Li and Carr<sup>26</sup> and Vailaya and Horváth<sup>27,28</sup> and is also found in our previous work.<sup>13</sup>

The second possibility, which we propose in this study, arises when the solvent has a homogeneous molecular structure dominated by one type of interaction. The solution properties represent the difference in interactions between solute and solvent states. A multicharacter nature not only affects the interaction between the solute and solvent molecules but also affects the interaction of solute liquid molecules. This latter effect often is overlooked. If the solvent is a homogeneous chemical compound such as squalane, only dispersion interactions occur in solution. Squalane is a hydrogenated, natural branched hydrocarbon commonly used in gas chromatography. With only dispersion interaction available, the solute–solvent interaction in squalane will be similar in magnitude for all solutes here. The solution thermodynamic properties in this solvent then represent largely the difference arising from solute liquid state interactions. Using this approach, the interaction of molecules in the solute liquid state can be investigated. Here, we have selected a number of derivatives with “dual character”.<sup>12</sup> Such molecules might be expected to assume selective orientation and contact with different structural units in the pure liquid state to affect solution thermodynamic properties. The possibility of observing entropy–enthalpy compensation then is studied here. Furthermore, a variation of the “group method” resulting from dividing a dual character molecule into a core and derivative group, will be extended to enthalpy and entropy of solution. At the functional group level, then entropy–enthalpy compensations may be observed even though both solute and solvent are multicharacter.

**TABLE 1: Calculated Entropies of Vaporization at normal Boiling Point ( $\Delta S_b^v$ ) and Solubility Parameters ( $\delta$ ) at 100 °C for Solutes Used Here**

solutes	$\Delta S_b^v$ (cal/K)	$\delta$ (cal <sup>0.5</sup> /cm <sup>1.5</sup> )
1. <i>n</i> -heptane	21.7	6.7
2. <i>n</i> -octane	22.0	6.8
3. <i>n</i> -nonane	22.3	6.9
4. benzene	21.6	8.3
5. toluene	21.7	8.1
6. <i>o</i> -xylene	22.0	8.1
7. 1-methyl-3-ethylbenzene	22.3	8.0
8. <i>n</i> -butyl acetate	23.0	7.7
9. cyclohexyl acetate	24.2	8.1
10. <i>m</i> -tolyl acetate	27.9	9.0
11. <i>p</i> -tolyl acetate	28.0	9.0
12. <i>n</i> -butyl TMSE	23.1	6.4
13. cyclohexyl TMSE	23.8	6.8
14. <i>m</i> -tolyl TMSE	25.2	7.2
15. <i>p</i> -tolyl TMSE	25.0	7.2
16. <i>n</i> -butyl TFA	23.7	6.9
17. cyclohexyl TFA	23.8	7.1
18. <i>m</i> -tolyl TFA	25.0	7.7
19. <i>p</i> -tolyl TFA	24.7	7.7
20. <i>n</i> -butyl PFP	23.4	6.4
21. cyclohexyl PFP	25.4	6.9
22. <i>m</i> -tolyl PFP	25.3	7.0
23. <i>p</i> -tolyl PFP	24.6	7.1
24. <i>n</i> -butyl <i>tert</i> -butyl ether	22.6	6.7

## 2. Experimental Section

The GLC equipment and procedure used for this study has been described earlier.<sup>12</sup> It can be noted that the gas chromatograph was “in house” constructed to maintain constant temperature. Columns were 0.5 cm in internal diameter and about 125 cm in length and contained at least 1.5 g of stationary phase on nonadsorbing supports. Five stationary phases were used: squalane, methoxy poly(ethylene oxide) (PEO), poly[methyl-(trifluoropropyl)siloxane] (QF-1), poly(methylphenyl) (DC-550), and poly(methylsiloxane) (DC-200). Stationary phases<sup>12,13</sup> and some solutes were purchased from commercial sources. Commercially unavailable solutes were synthesized and have been reported earlier with their vapor pressures.<sup>29</sup> The entropy of vaporization of solutes at normal boiling point (Trouton Number) and the solubility parameters at 100 °C were calculated from vapor pressures, using the Clausius–Clapeyron equation<sup>30</sup> and are shown in Table 1. Measurements of retention volumes were made in triplicate at 80 and 100 °C. Helium was used as the carrier gas. From the specific retention volumes, the Flory–Huggins interaction parameters,  $\chi$ , were determined using the established equation.<sup>10–15</sup>

In the original Flory–Huggins treatment,<sup>31–33</sup> the interaction parameter,  $\chi$ , was a constant contact energy difference between solute and solvent. However, experience has shown that  $\chi$  usually depends on temperature.<sup>33,34</sup> Guggenheim<sup>35</sup> suggested that  $\chi$ , the free energy of contact, be separated so that

$$\chi = \chi_H + \chi_S \quad (2)$$

where the reduced excess enthalpy of solution,  $\chi_H$ , and reduced residual entropy of solution,  $\chi_S$ , are defined as

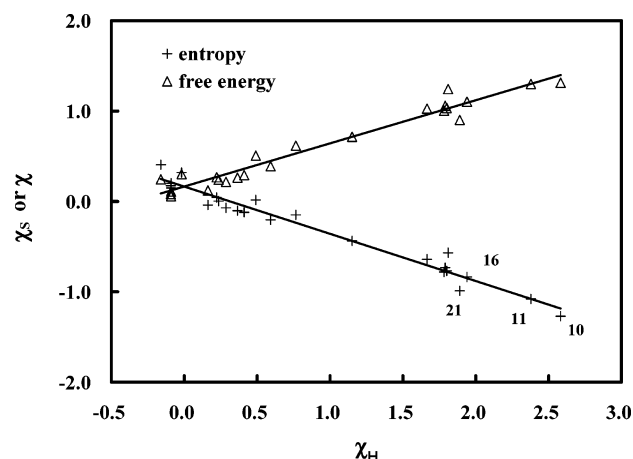
$$\chi_H = -T \left( \frac{\partial \chi}{\partial T} \right) = \Delta \bar{H}_e^\infty / RT \quad (3)$$

$$\chi_S = \frac{\partial(T\chi)}{\partial T} = -\Delta \bar{S}_{re}^\infty / R \quad (4)$$

Here  $T$  is the absolute temperature,  $R$  is the gas constant,  $\Delta \bar{H}_e^\infty$

**TABLE 2: Slopes and Correlation Coefficients (*R*) of  $\chi_S$  vs  $\chi_H$  and  $\chi$  vs  $\chi_H$  Plots in Stationary Phases of This Study at 90 °C**

stationary phases	$\chi_S$ vs $\chi_H$		$\chi$ vs $\chi_H$	
	slope	<i>R</i>	slope	<i>R</i>
squalane	−0.5225	0.9813	0.4775	0.9773
PEO	−0.4833	0.9328	0.5167	0.9405
QF-1	−0.3305	0.6314	0.6695	0.8552
DC-550	−0.5964	0.9308	0.4036	0.8649
DC-200	−0.5709	0.8936	0.4291	0.8315

**Figure 1.** Reduced residual entropy ( $\chi_S$ ) and reduced size corrected free energy ( $\chi$ ) vs reduced excess enthalpy ( $\chi_H$ ) of solutes in dilute solution in squalane at 90 °C. Lines are linear least-squares plots for all solutes. (See Table 1 for solute codes.)

is excess enthalpy of solution, and  $\Delta\tilde{S}_{re}^\infty$  is the residual entropy of solution or the noncombinatorial part of the entropy of solution.  $\Delta\tilde{S}_{re}^\infty$  is associated with solute–solvent interaction. The residual enthalpy is generally considered to be the excess enthalpy of solution. It was noted earlier<sup>12</sup> that the size correction gives a contribution to the entropy of solution but there is no counterpart in the enthalpy of solution. Therefore, in making an entropy–enthalpy plot the sized corrected result should be used.

### 3. Results and Discussion

**3.1. Solute State Interactions.** Experimental values of reduced size corrected free energy of solution ( $\chi$ ) at 80 and 100 °C, reduced excess enthalpy ( $\chi_H$ ), reduced residual entropy ( $\chi_S$ ), of 24 solutes at 90 °C in the five solvents studied here have been reported earlier.<sup>12,13</sup> For some solutes, data were not measured for 80 °C because of lengthy retention time; for these, high-temperature data<sup>36,37</sup> were used to obtain  $\Delta\tilde{H}_e^\infty$  and  $\Delta\tilde{S}_{re}^\infty$ , and results were adjusted to 90 °C using eq 3. The slopes and correlation coefficients (*R*) of  $\chi_S$  vs  $\chi_H$ , and  $\chi$  vs  $\chi_H$  plots were determined and results are shown in Table 2. Here, we can note that for squalane and PEO, data are better correlated than with other solvents.

Figure 1 shows the plot of  $\chi_S$  vs  $\chi_H$  and  $\chi$  vs  $\chi_H$  for solutes in squalane. It can be seen that there is a good correlation between entropy and enthalpy of solution and the correlation is equally good for the  $\chi$  vs  $\chi_H$  plot. The values of  $\chi_H$  range from small negative to positive values. In squalane, there are only weak alkyl interactions with solutes; a large portion of positive  $\chi_H$  values represents the difference between pure solute liquid state interactions and the interactions with squalane. The data relating free energy and entropy to enthalpy are both well correlated with a linear relationship. The slope of the  $\chi_S$  vs  $\chi_H$

line was about −0.52, which indicates that the entropy components contribute about half the value of  $\chi$  compared to the enthalpy. Furthermore, the slope differs from unity; therefore, the compensation temperature is far from the experimental temperature and the system is not highly compensated. It was emphasized by Krug et al.<sup>36</sup> that the correlation would not be significant at the 95% confidence level if the compensation temperature lies within two standard deviations of the experimental temperature. The standard deviations for the slopes of plots in Table 2 are less than 0.1; therefore, all compensation temperatures differ from the experimental temperature.

Selected solutes with high  $\chi_H$  are identified in Figure 1. The solutes with the highest  $\chi_H$  values are two tolyl acetates (10 and 11), where attractive intermolecular interaction exists between acetate groups and aromatic rings in the solute liquid state. During the dissolution process into squalane, more energy was required to separate the solute molecules than was released during the solution process, resulting in a positive  $\chi_H$  for the overall solution process. The third and fourth highest  $\chi_H$  values are for *n*-butyl TFA (16) and cyclohexyl PFP (21), respectively. These two solutes in the liquid state do not involve attractive polar moieties. Rather, a high value of  $\chi_H$  represents the disruption of favorable intermolecular fluorocarbon–fluorocarbon interactions, which exist in the solute liquid state but are replaced by unfavorable alkane–fluorocarbon interactions in squalane solution. In this respect, the positive  $\chi_H$  values for alkyl fluoroesters result from repulsive forces in the solvent rather than attractive interactions in the liquid solute. It is noteworthy that both attractive interaction of tolyl acetates and repulsive interaction of alkyl fluoroesters were well correlated by a single line with the homogeneous solvent.

Other evidence for identifying interaction mechanisms between pure tolyl acetates and alkyl fluoroesters comes from the solubility parameters and entropies of vaporization shown in Table 1. The solubility parameter is the square root of cohesive energy density, which represents the energy required to separate molecular liquids into their ideal gaseous state.<sup>38</sup> For tolyl acetates, the solubility parameters are much higher than for alkyl fluoroesters, where values are close to those of hydrocarbons. This would suggest that there is little attractive interaction between the moieties of alkyl fluoroesters beyond the level of alkyl–alkyl interactions. The entropy of vaporization also indicates that there is more organizational order for tolyl acetates and alkyl fluoroesters in the solute liquid state than in an *n*-alkane liquid. Furthermore, in both types of interactions  $\chi_S$  is negative during the solution process, representing a positive  $\Delta\tilde{S}_{re}^\infty$  and randomness increase exceeding that of an ideal solution, in agreement with the mechanistic explanation presented here.

Figure 2 shows a plot similar to that of Figure 1 for PEO. For PEO, the solute–solvent interaction differs significantly from that of squalane; PEO involves a strong polar environment. When solute molecules do not interact strongly with solvent at the level of PEO, a positive  $\chi_H$  will result. The solutes with higher  $\chi_H$  values now are *n*-alkanes (1–3) followed by *n*-butyl ethers (12 and 21). Solute state interaction provides some decrease in  $\chi_H$  values for some solutes such as tolyl TFA (18 and 19) and possibly tolyl acetates. The results for the  $\chi_S$  and  $\chi_H$  for tolyl acetates were not available because of lengthy 80 °C retention volumes. The values of  $\chi$  at 100 °C are very low at 0.068 and 0.043 for *m*-tolyl acetate and *p*-tolyl acetate, respectively.<sup>12</sup> On the basis of the correlation of the  $\chi$  vs  $\chi_H$  line in Figure 2, these values will give a negative  $\chi_H$  and place them on the left-hand side of the other solutes. The slope for



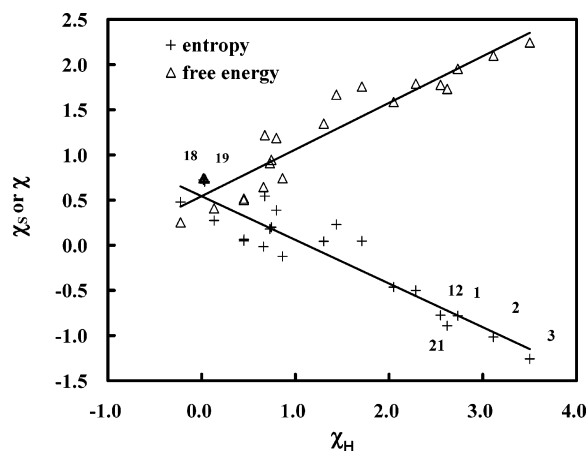


**Figure 2.** Reduced residual entropy ( $\chi_S$ ) and reduced size corrected free energy ( $\chi$ ) vs reduced excess enthalpy ( $\chi_H$ ) of solutes in PEO at 90 °C. Lines are linear least-squares plots for all solutes in dilute solution. (See Table 1 for solute codes.)

the  $\chi_S$  vs  $\chi_H$  plot is  $-0.48$ ; despite the strong polar solvent atmosphere, the slope is similar to that of Figure 1. For PEO, the  $\chi$  vs  $\chi_H$  plot shows a higher correlation,  $R$ , than the  $\chi_S$  vs  $\chi_H$  plot. A further comparison for other solute–solvent systems shown in Table 2 and later in Tables 4 and 6 showed that the sum of the absolute values of the two slopes is unity. In addition, when the  $\chi$  vs  $\chi_H$  plot has a slope higher than 0.5, there are higher  $R$  values for  $\chi$  vs  $\chi_H$  plots. This is because when the slope is higher than 0.5, the spread of  $\chi$  values is higher than that for  $\chi_S$  values, and this consequently leads to a higher correlation.

In Table 2, it can be seen that for the three other solvents, DC-200, DC-550, and QF-1, plots gave lower correlation coefficient values. The plots of  $\chi_S$  vs  $\chi_H$  for these three solvents are quite scattered and are not shown here. It is of interest to consider a reason for the linearity for squalane and PEO plots and the absence of linearity for the other three solvents. The explanation for the linearity is because squalane and PEO are solvents providing relatively homogeneous environments. When a solute is dissolved into squalane or PEO, the pure solute liquid environment is replaced by the infinite dilution state in the solvent. In the solvent, the interaction tends to be homogeneous and the interaction between solvent and different moieties of solutes is of a similar type. A large portion of the difference in  $\chi_S$  and  $\chi_H$  is a result of the difference in separating the solute molecules from their liquid state. Therefore, the slopes of  $\chi_S$  vs  $\chi_H$  and  $\chi$  vs  $\chi_H$  for these two solvents are similar. The solute can be multifunctional, but it is seen here that the separation of these molecules and insertion into a homogeneous solvent environment has entropy–enthalpy compensation consequences.

Though not always recognized, silicones DC-200, DC-550, and QF-1 are essentially multicharacter solvents. Various solute molecule moieties selectively can contact various solvent molecule functional groups to reduce solution enthalpy. This would make for lower  $\chi_H$  values in a process accompanied by a lower solution entropy than might occur otherwise because of the reduced freedom of functional groups to participate in the interaction. Although this process is in physical agreement with the description from eq 1, the result is that there are many possible combinations in solute liquids as well as in solutions that can cause the plot of overall enthalpy and entropy of solution to deviate from linearity. Another consequence of selective contacting between functional groups is that there is a narrow range of  $\chi_H$  and  $\chi_S$  values in comparison to solutions involving squalane and PEO. A wide range of  $\chi$  and  $\chi_H$  is useful

in separating different solutes. This would make a homogeneous stationary phase with a solubility parameter substantially different from the solutes a better choice for separation.<sup>39</sup>

### 3.2. Enthalpy and Entropy of Transfer between Solvents.

A chromatographic process involves a partitioning of a solute between a mobile and a stationary phase. For instance, in GLC the retention volume is a measure of the partitioning of solutes between a mobile carrier gas and an immobilized supported solvent in a column. At equilibrium, the chemical potential of the solute is the same in both the carrier gas and the solvent. When a different solvent is used under similar conditions, the retention volumes for any given solute in two different solvents can be related directly to the partition coefficient of that solute in the two solvents, which are not in contact with each other. Therefore, gas chromatography has been proposed as a means for obtaining information for the design of separation processes based on partitioning and solution effects.<sup>40</sup> Two important examples would be liquid–liquid extraction and liquid–liquid chromatography. Assuming in liquid–liquid extraction a solute is partitioned between two immiscible liquid phases, “a” and “b”, at equilibrium the chemical potentials in the two phases are the same; then

$$x_a \gamma_a = x_b \gamma_b \quad (5)$$

and

$$x_a/x_b = \gamma_b/\gamma_a = V_a/V_b \exp(\chi_b - \chi_a) \quad (6)$$

where  $x$  are indicated mole fractions,  $\gamma$  are activity coefficients in designated solvents, and  $V_a/V_b$  is the ratio of the molar volume of two solvents. In the last term of eq 6 the Flory–Huggins equation was employed and the molecular weights of the two solvents were assumed to be much higher than those of the solutes. The ratio of molar volumes is not convenient when the molecular volumes of the solvents are not known accurately, but this can be overcome with the use of the weight fraction ratio,  $w_a/w_b$ . From the above equations and the relationship between the activity coefficient and retention volumes of GLC, Sheehan and Langer<sup>40</sup> showed that the weight fraction ratio can be related to the ratio of the specific chromatographic retention volumes for the two solvents,  $V_{g,a}^T/V_{g,b}^T$ :

$$w_a/w_b = V_{g,a}^T/V_{g,b}^T = (\rho_a/\rho_b) \exp(\chi_b - \chi_a) \quad (7)$$

where  $\rho_a/\rho_b$  is the density ratio of the solvents. Therefore, the partition coefficient of a solute between two phases is related to the relative concentration of a solute in the two phases. Both  $x_a/x_b$  and  $w_a/w_b$  can be treated as the partition coefficient.<sup>41</sup> The logarithm of the partition coefficients is related to the difference of reduced size corrected free energy of solution,  $\chi_b - \chi_a$ . This quantity is a measure of the free energy change of transfer. From the partition coefficient variation with temperature, the enthalpy and entropy of transfer can also be obtained. Because the solute molecules are compared at infinite dilution in two solvents, the pure solute state interactions are subtracted in the calculation of the thermodynamic properties of transfer.

In another sense, a solution process can also be considered as a transfer process from a solute liquid to a solvent. It can now be understood why it is more difficult to observe entropy–enthalpy compensation in solution processes compared to chemical kinetic processes. This is because the solute liquid state is different for each solute. But when transfer properties are considered, each solvent provides a similar environment for solutes, particularly in the results obtained from GLC, which

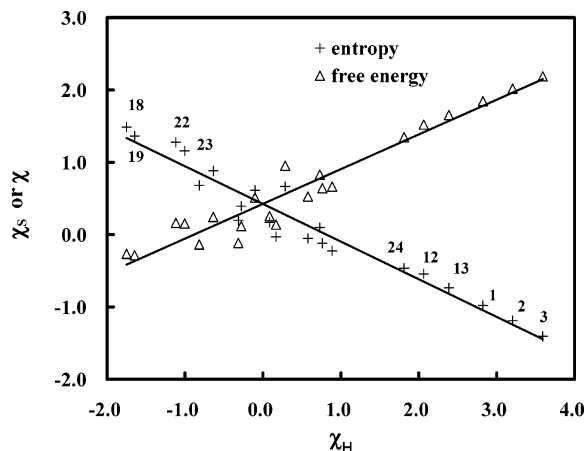


**Figure 3.** Reduced residual entropy ( $\chi_s$ ) and reduced size corrected free energy ( $\chi$ ) vs reduced excess enthalpy ( $\chi_H$ ) of transfer for solutes from squalane to PEO at 90 °C. Lines are linear least-squares plots for all solutes in dilute solution. (See Table 1 for solute codes.)

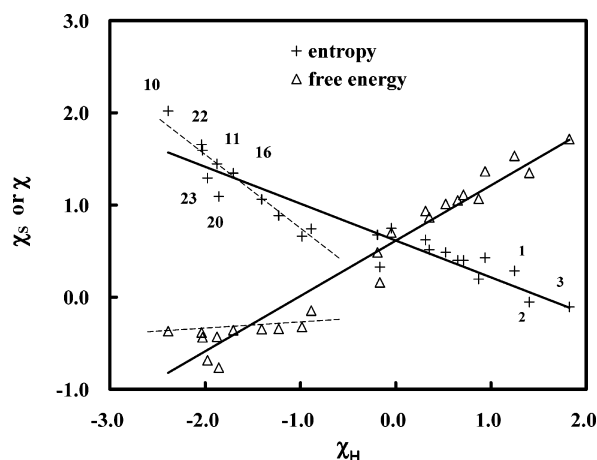


**Figure 4.** Reduced residual entropy ( $\chi_s$ ) and reduced size corrected free energy ( $\chi$ ) vs reduced excess enthalpy ( $\chi_H$ ) of transfer for solutes from squalane to QF-1 at 90 °C. Solid lines are linear least-squares plots for all solutes in dilute solution. Dashed lines are drawn to show another trend (see text). (See Table 1 for solute codes.)

usually involves infinite dilute solutions, and consideration of the pure liquid solute state is minimal. Therefore, there is the possibility that entropy–enthalpy compensation effects might be observed through examination of transfer properties. When the transfer properties between two solvents are considered, most of the free volume effects<sup>3,13,42</sup> between volatile solute and nonvolatile solvents are also canceled. This is because all solutes are considered to have the same reduced volume as the solvent in an infinite dilute solution.

Figure 3 shows the entropy–enthalpy plot of transfer from squalane to PEO, and Figures 4–6 shows that for transfer to QF-1, DC-550, and DC-200, respectively. Squalane is used as the reference because as a hydrocarbon it is free from specific interactions. The corresponding slopes and  $R$  values are shown in Table 4. It can be seen in Figure 3 that the correlation is higher than solution into PEO in Figure 2, whereas for QF-1 and DC-550 the correlation coefficients (from Table 4) are also much higher than solution into polymers in Table 2. In contrast, DC-200 showed a decrease in  $R$ . In Figure 3, the range of  $\chi_H$  values is wider than that in Figure 2. At the right-hand side of the range are  $n$ -alkanes and several ethers. The values of  $\chi_H$  are positive because these solutes are nonpolar or only slightly polar. The  $\chi$  value is also positive in contrast to negative  $\chi_s$ . This means these solutes favor squalane over PEO. At the left-

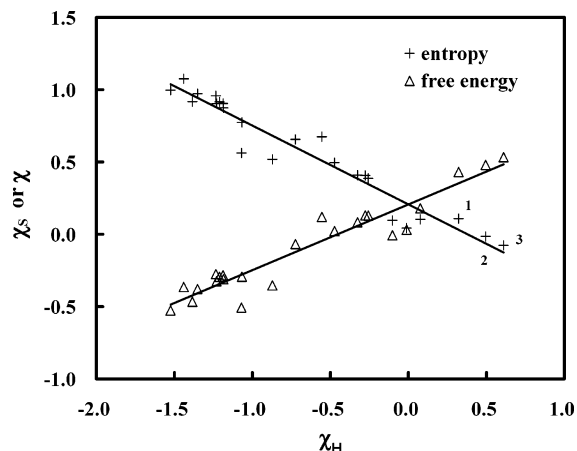


**Figure 5.** Reduced residual entropy ( $\chi_s$ ) and reduced size corrected free energy ( $\chi$ ) vs reduced excess enthalpy ( $\chi_H$ ) of transfer for solutes from squalane to DC-550 at 90 °C. Lines are linear least-squares plots for all solutes in dilute solution. (See Table 1 for solute codes.)

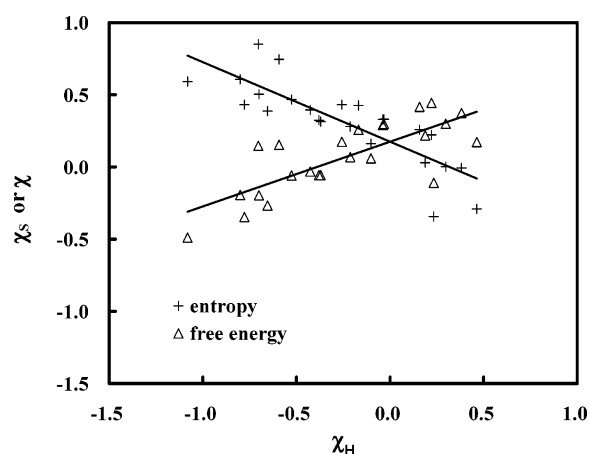


**Figure 6.** Reduced residual entropy ( $\chi_s$ ) and reduced size corrected free energy ( $\chi$ ) vs reduced excess enthalpy ( $\chi_H$ ) of transfer for solutes from squalane to DC-200 at 90 °C. Lines are linear least-squares plots for all solutes in dilute solution. (See Table 1 for solute codes.)

hand side are aromatic esters containing two moieties that can both interact with PEO. The varying interaction strengths of solutes give a range of negative values for  $\chi_H$ , but the accompanying positive  $\chi_s$  results in a total  $\chi$  that is only slightly negative. The overall result is that solutes at the left-hand side of the distribution somewhat favor PEO.

Figure 4 shows the enthalpy and entropy of transfer from squalane to QF-1. The overall data show that  $\chi_H$  is lower whereas  $\chi_s$  is higher than in Figure 3. With the exception of two solutes at the right end, the values of  $\chi_s$  are all positive. Despite the high correlation coefficient, these data do not provide a simple linear pattern.  $n$ -Alkanes give positive  $\chi_H$  values upon transfer to QF-1, but these values are less than in Figure 3. This is because QF-1 does contain some alkyl substituents in the siloxane chains,<sup>13,43</sup> which provide more favorable interaction with  $n$ -alkanes than with PEO. The data points with negative  $\chi_H$  can be correlated using another line and are shown as dashed lines in Figure 4. These solutes have a more negative slope in the  $\chi_s$  vs  $\chi_H$  line but render  $\chi$  negative and almost constant. These ester solutes fall into the “dual character” category.

Because relative values are used in transfer property comparisons, they do not include solute liquid state interaction. Furthermore, specific interactions are absent in squalane. This leaves QF-1 the only source for the second correlation at the left-hand side of Figure 4. The occurrence of these two

**TABLE 3: Reduced Residual Enthalpy of Transfer ( $\chi_H$ ) and Reduced Residual Entropy of transfer ( $\chi_S$ ) for Solutes from Squalane to Polymers at 90 °C**

solutes	squalane–PEO		squalane–QF-1		squalane–DC5		squalane–DC200	
	$\chi_H$	$\chi_S$	$\chi_H$	$\chi_S$	$\chi_H$	$\chi_S$	$\chi_H$	$\chi_S$
1. <i>n</i> -heptane	2.824	−0.980	0.937	0.428	0.322	0.109	0.188	0.030
2. <i>n</i> -octane	3.206	−1.190	1.246	0.286	0.495	−0.015	0.297	0.002
3. <i>n</i> -nonane	3.593	−1.406	1.821	−0.105	0.610	−0.076	0.381	−0.007
4. benzene	−0.817	0.681	−0.191	0.676	−0.724	0.656	−0.257	0.431
5. toluene	−0.277	0.394	−0.047	0.748	−0.474	0.496	−0.039	0.329
6. <i>o</i> -xylene	0.087	0.168	0.352	0.514	−0.326	0.409	0.158	0.258
7. 1-methyl-3-ethylbenzene	0.578	−0.053	0.710	0.399	−0.257	0.386	0.221	0.222
8. <i>n</i> -butyl acetate	−0.314	0.198	−0.888	0.742	−1.351	0.972	−0.371	0.314
9. cyclohexyl acetate	0.169	−0.031	−0.167	0.327	−0.872	0.518	−0.102	0.161
10. <i>m</i> -tolyl acetate	<i>a</i>	<i>a</i>	−2.388	2.019	−1.524	0.997	−0.703	0.850
11. <i>p</i> -tolyl acetate	<i>a</i>	<i>a</i>	−2.039	1.655	−1.070	0.562	−0.593	0.746
12. <i>n</i> -butyl TMSE	2.064	−0.543	0.650	0.400	−0.276	0.407	−0.426	0.395
13. cyclohexyl TMSE	2.388	−0.735	1.401	−0.052	0.076	0.104	0.463	−0.290
14. <i>m</i> -tolyl TMSE	0.762	−0.120	0.313	0.622	−0.103	0.096	−0.169	0.426
15. <i>p</i> -tolyl TMSE	0.889	−0.226	0.524	0.487	−0.012	0.043	−0.033	0.330
16. <i>n</i> -butyl TFA	−0.637	0.881	−1.977	1.292	−1.385	0.918	−0.778	0.431
17. cyclohexyl TFA	0.286	0.666	−0.985	0.661	−1.230	0.904	0.233	−0.343
18. <i>m</i> -tolyl TFA	−1.750	1.485	−1.705	1.347	−1.210	0.916	−0.526	0.467
19. <i>p</i> -tolyl TFA	−1.648	1.362	−1.407	1.061	−1.067	0.774	−0.380	0.323
20. <i>n</i> -butyl PFP	−0.100	0.613	−1.857	1.092	−1.440	1.075	−1.081	0.591
21. cyclohexyl PFP	0.730	0.098	−1.229	0.885	−1.186	0.875	−0.654	0.387
22. <i>m</i> -tolyl PFP	−1.117	1.278	−2.028	1.593	−1.234	0.958	−0.801	0.607
23. <i>p</i> -tolyl PFP	−1.003	1.156	−1.876	1.446	−1.188	0.905	−0.700	0.504
24. <i>n</i> -butyl <i>tert</i> -butyl ether	1.812	−0.466	0.870	0.196	−0.555	0.675	−0.213	0.280

<sup>a</sup> Retention volume was measured only for 100 °C.

**TABLE 4: Slopes and Correlation Coefficients (*R*) of  $\chi_S$  vs  $\chi_H$  and  $\chi$  vs  $\chi_H$  Plots for Transfer Properties in Dilute Solution from Squalane to Polymers at 90 °C**

stationary phases	$\chi_S$ vs $\chi_H$		$\chi$ vs $\chi_H$	
	slope	<i>R</i>	slope	<i>R</i>
PEO	−0.5202	0.9701	0.4798	0.9651
QF-1	−0.3998	0.9372	0.6002	0.9706
DC-550	−0.5453	0.9661	0.4547	0.9523
DC-200	−0.5514	0.8319	0.4486	0.7734

correlation lines can be explained through the dual character nature of QF-1. QF-1 consists of fluorocarbon units and alkyl units attached to the siloxane chain.<sup>13,43</sup> In the pure solvent, the fluorocarbon groups probably contact similar partners to minimize energy, resulting in a more ordered liquid structure. When a dual character solute molecule such as *n*-butyl PFP dissolves in the solvent matrix, it is probably incorporated within the solvent structure and localized so that the *n*-butyl group contacts the alkyl region and the PFP group contacts fluorocarbon groups minimizing energy. This process decreases  $\chi_H$  of transfer, but the simultaneous localization of two moieties within the solvent structure produces a large entropy decrease and more positive  $\chi_S$  value. In contrast, *n*-alkanes and ether molecules probably favor the alkyl region without simultaneously contacting the fluorocarbon region. This results in less effect on  $\chi_S$  values; therefore, the  $\chi_S$  vs  $\chi_H$  line gives a lower negative slope. For these solutes  $\chi_H$  and  $\chi$  are more positive, as seen in Figure 4. This illustrates the role of dual character in affecting solution as well as transfer properties.

Figure 5 shows the  $\chi_H$  vs  $\chi_S$  plot of transfer for solutes from squalane to DC-550. The corresponding plot for DC-200 is shown in Figure 6. Reduced excess enthalpies,  $\chi_H$ , of *n*-alkanes in Figure 5 are positive because interactions with DC-550 involves phenyl groups that have less favorable aromatic–alkane contacts in solution. This makes the transfer of *n*-alkanes from squalane to DC-550 less favorable. For most other solutes the distribution in DC-550 is more favorable because of the phenyl group, which provides attractive solute interactions. This is

similar to the previously noted situation in QF-1 except that in DC-550 the dual character nature is weaker so that a single line can correlate all solutes. In Figure 6, there are more solutes with positive  $\chi_H$  and  $\chi$  values compared to Figure 5. This is because silicone DC-200 contains only methyl substituents. This very limited DC-200 multifunctional character results in less compatibility with nonalkane solutes. The range of  $\chi_H$  values in Figure 5 is narrower than in Figure 4. The range of values in Figure 6 in turn is narrower than that in Figure 5. The range of  $\chi$  and  $\chi_H$  for transfer properties is amenable to estimation from the solubility parameter model<sup>38</sup> where it is assumed that  $\chi$  can be estimated with the solute molar volume, *V*, and the solubility parameters of solute,  $\delta$ , and solvent,  $\delta_a$ , using the equation

$$\chi = V(\delta - \delta_a)^2/RT \quad (8)$$

When transfer properties between two solvents “a” and “b” are considered,

$$\chi_a - \chi_b = V(\delta_a - \delta_b)(\delta_a + \delta_b - 2\delta)/RT \quad (9)$$

Therefore, the solubility parameter difference for two solvents,  $\delta_a - \delta_b$ , can provide an estimate of the range of  $\chi_a - \chi_b$  values. Through the linear relationships,  $\chi_{H,a} - \chi_{H,b}$  and  $\chi_{S,a} - \chi_{S,b}$  are also proportional to the difference in the solubility parameters of two solvents. The solubility parameters of QF-1<sup>43</sup> and PEO<sup>44</sup> are much higher than that for squalane, a saturated hydrocarbon. The solubility parameters of DC-200 and DC-550<sup>45</sup> are much closer to hydrocarbon values. The narrow range of  $\chi_H$  values in Figure 6 makes the deviation from a linear trend important and accounts for the smaller correlation coefficient for DC-200. This also explains why the transfer properties of DC-200 have a lower *R* value than the solution properties. This is because the transfer properties were weighted by a small  $(\delta_a - \delta_b)$  in eq 9 whereas the solution properties vary with the solubility parameter of solutes, as shown in eq 8. Compared to Figure 6, the transfer into DC-550 is also characterized by a higher  $\chi_S$  for many ester solutes, which can arise from the increase in

**TABLE 5: Contributions of Hydrocarbon Cores and Derivatizing Groups to the Reduced Enthalpy ( $\chi_H$ ) and Residual Entropy ( $\chi_S$ ) of Transfer in Dilute Solution from Squalane to Polymers at 90 °C**

solutes	squalane-PEO		squalane-QF-1		squalane-DC550		squalane-DC200	
	$\chi_H$	$\chi_S$	$\chi_H$	$\chi_S$	$\chi_H$	$\chi_S$	$\chi_H$	$\chi_S$
1. <i>n</i> -butyl	1.604	-0.596	0.667	0.101	0.238	0.003	0.144	0.004
2. cyclohexyl	2.244	-0.884	1.441	-0.325	0.548	-0.240	0.794	-0.450
3. <i>m</i> -tolyl	0.649	-0.003	0.233	0.615	0.333	-0.098	0.259	0.159
4. <i>p</i> -tolyl	0.763	-0.120	0.486	0.382	0.517	-0.269	0.382	0.047
5. acetate	-1.388	0.484	-2.077	0.993	-1.613	0.914	-0.837	0.578
6. TMSE	0.211	-0.005	0.015	0.171	-0.488	0.314	-0.436	0.275
7. TFA	-2.252	1.499	-2.225	0.897	-1.632	1.029	-0.757	0.280
8. PFP	-1.688	1.187	-2.454	1.061	-1.671	1.105	-1.204	0.582
9. <i>tert</i> -butoxyl	0.208	0.130	0.203	0.095	-0.793	0.672	-0.357	0.276

order when they are localized within the DC-550 structure. However, compared to QF-1 in Figure 4, which involves a strong fluorocarbon-fluorocarbon interaction, the values of  $\chi_S$  in Figure 5 are smaller than those of Figure 4.

### 3.3. Group Effects on Enthalpy and Entropy of Transfer.

The derivatives here include four parent type compounds: *n*-butyl, cyclohexyl, *m*-tolyl, and *p*-tolyl groups, with four types of derivatizing agents including acetates, TMSE's, TFA's, and PFP's. *n*-Butyl *tert*-butyl ether was included because of its structural similarity to *n*-butyl TSME. Indeed, the solution properties of the latter pair are similar. For "dual character" solutes, simple linear relations between excess properties can be distorted by the complexities arising from a variety of solution interactions and orientations. Here, we now attempt to separate molecules into large component moieties so that entropy-enthalpy compensation might be more readily examined. Earlier we proposed considering solute molecules as combinations of moieties.<sup>13</sup> The use of a "group contribution method" to calculate free energies of solution and activity coefficients has a long history.<sup>30,46,47</sup> Most earlier studies attempt to separate molecules into their most basic structural units. Here, a different approach is used because the objective is to show an entropy-enthalpy compensation with minimal molecular division. Thus, molecules are treated as consisting of two parts—a hydrocarbon core and a "derivative group".

The group effect on  $\chi$  was studied earlier.<sup>13</sup> Here a similar approach is used for  $\chi_H$  and  $\chi_S$ . The  $\chi$  value of the first hydrocarbon core is determined from the three *n*-alkanes used. Because  $\chi_H$  and  $\chi_S$  are linear with respect to carbon number, the linear regression result for *n*-octane was treated as the sum of two *n*-butyl groups. Other hydrocarbon cores were calculated on the basis of the difference of  $\chi_H$  values relative to *n*-butyl groups. For example, the difference between four *n*-butyl derivatives and cyclohexyl derivatives were averaged and from this value the  $\chi_H$  of the cyclohexyl core was determined. After hydrocarbon cores were determined,  $\chi_H$  values of derivatizing groups were calculated from solutes of the same derivative by subtracting the contribution of hydrocarbon cores. For most derivatives, the averages were taken for four hydroxyl compounds. The effect of the *tert*-butoxyl group was determined from the difference of  $\chi_H$  between *n*-butyl *tert*-butyl ether and the *n*-butyl group. The effects of hydrocarbon cores and derivatizing groups on  $\chi_H$  and  $\chi_S$  values of transfer between squalane and polymers at 90 °C are shown in Table 5. The plot to test for entropy-enthalpy compensation of these groups is shown in Figure 7. The slopes and correlation coefficients are shown in Table 6. Overall, the correlations are quite good for these groups.

In Figure 7, PEO has the widest range of group properties followed by QF-1, then DC-550 and DC-200. This reflects closely the ranges of Figures 3–6. Three esters, acetate, TFA,

**TABLE 6: Slopes and Correlation Coefficients of  $\chi_S$  vs  $\chi_H$  and  $\chi$  vs  $\chi_H$  Plots for Dilute Solution in Stationary Phases of This Work at 90 °C**

stationary phases	$\chi_S$ vs $\chi_H$		$\chi$ vs $\chi_H$	
	slope	<i>R</i>	slope	<i>R</i>
PEO	-0.4923	0.9735	0.5077	0.9750
QF-1	-0.3051	0.9201	0.6949	0.9830
DC-550	-0.5784	0.9921	0.4216	0.9853
DC-200	-0.4888	0.9100	0.5112	0.9167

and PFP, are placed on the far left-hand side of each line in Figure 7 because they interact with oxygenated solvents better than squalane. Both PEO and QF-1 separated ester groups and hydrocarbon groups more widely. PEO is very selective toward the three ester groups with TFA the most negative followed by PFP and acetate. The differences caused by fluoromethylene units also are most prominent in the polar PEO phase. Because fluorocarbon units are unfavorable in either squalane or PEO, the overall result in transfer properties is a relative difference between two solvents. In a transfer from squalane to PEO, the fluoromethylene unit in TFA and PFP introduced unfavorable interactions with PEO, causing  $\chi_H$  and  $\chi$  to increase. An additional fluoromethylene unit now leads to considerable unfavorable interaction, as indicated through the differences between TFA and PFP. QF-1 is known to interact with ester groups.<sup>48</sup> This was true with acetates and even stronger with TFA and PFP. QF-1 also gives good separations for the three esters. This is one consequence of the favorable interaction between solute fluoromethylene units and the solvent. In QF-1, PFP is the most negative because of the additional fluorocarbon group interaction. Groups in QF-1 also have a higher

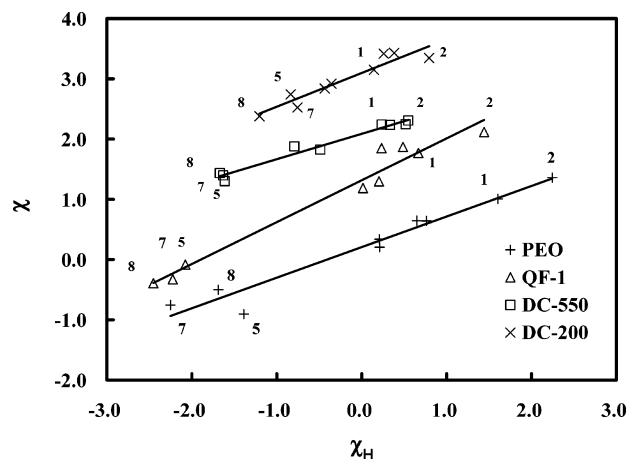


**Figure 7.** Group effects on reduced sized corrected free energy ( $\chi$ ) and reduced enthalpy ( $\chi_H$ ) of transfer for solutes from squalane to polymers at 90 °C. Data for QF-1, DC-550, and DC-200 were shifted upward by 1.0, 2.0, and 3.0, respectively. Lines are linear least-squares plots for all groups. (See Table 6 for group codes.)



slope than in other solvents. This reflects the fact that when esters dissolve in QF-1 either  $\chi_S$  is particularly negative or  $\chi_H$  is more positive compared to other groups. Ether groups are placed on the right-hand side with hydrocarbon cores. A combination of one ester group with a hydrocarbon core gives a different slope for entropy–enthalpy correlation, accounting for the second line in Figure 4.

On the right-hand side of each line is the cyclohexyl group. The cyclohexyl group has higher  $\chi_H$  and lower  $\chi_S$  values than the *n*-butyl group. The difference in values of  $\chi_H$  and  $\chi_S$  between the cyclohexyl group and *n*-butyl group are equivalent to about two methylene units, i.e., the difference between *n*-heptane and *n*-nonane in Table 3. It can be noted that the cyclohexyl group contains 6 carbon atoms, albeit in a ring. Both cyclohexyl and *n*-butyl groups are alkyl type groups in terms of interaction, and an entropy–enthalpy compensation is observed for the effect of size increase and changing geometry. The difference between *m*- and *p*-phenyl groups is small. *m*-Phenyl has a higher  $\chi_H$ , but this is compensated by lower  $\chi_S$ . This would indicate that there is some entropy–enthalpy compensation for isomers with solvent variation. Finally, the difference between the effect of *tert*-butoxyl and TMSE was also small in the transfer from squalane to PEO. Differences are higher for the transfer from squalane to dual character silicones QF-1, DC-550, and DC-200. This again indicates some entropy–enthalpy compensation for this group pair in related dual character solvents.

#### 4. Conclusions

From Flory–Huggins parameters,  $\chi$ , obtained through GLC measurements, the reduced excess enthalpy of solution,  $\chi_H$ , and reduced residual entropy of solution,  $\chi_S$ , of a variety of solutes in squalane, several silicone type polymeric solvents, and PEO are examined. A variety of derivatives, consisting of molecules of two groups of disparate properties (dual character), exhibit trends in solution thermodynamic properties. These trends can be related somewhat to the solvent and solute structures, and the nature of the solution processes. Entropy–enthalpy compensation was observed for solution in squalane and PEO. The distribution between two solvents also calculated for selected solvent pairs at infinite dilution showed additional entropy–enthalpy compensation effects. For derivatives, the enthalpy and entropy of transfer were shown to be amenable to structural unit type summation treatment. The effect of groups on enthalpy and entropy also show an entropy–enthalpy compensation. This work, based on careful gas chromatographic measurements, demonstrates once more how these measurements can be valuable for interpreting and studying solution phenomena at high dilution in high molecular weight and polymeric liquids.

**Acknowledgment.** We thank the reviewer for helpful comments and suggestions.

**Note Added after ASAP Publication.** This article was published on the Web on 1/19/2005. A change has been made in the title. The correct version was posted on 1/21/2005.

#### References and Notes

(1) Conder, J. R.; Young, C. L. *Physicochemical Measurements by Gas Chromatography*; Wiley: New York, 1979.

- (2) Laub, R. J.; Pecsok, P. L. *Physicochemical Applications of Gas Chromatography*; Wiley: New York, 1979.
- (3) Vilcu, R.; Leca, M. *Polymer Thermodynamics by Gas Chromatography*; Vasilescu, V., Translator; Elsevier: Amsterdam, 1990.
- (4) Al-Saigh, A. Z. *Polym. News* **1994**, 19, 269–279.
- (5) Gray, D. G.; Guillet, J. E. *Macromolecules* **1973**, 6, 223–227.
- (6) Romansky, M.; Guillet, J. E. *Polymer* **1994**, 35, 586–589.
- (7) Guillet, J. E. In *New Development in Gas Chromatography*; Purnell, J. H., Ed.; Wiley: New York, 1979; p 187.
- (8) Thede, R.; Below, E.; Haberland, D.; Langer, S. H. *Chromatographia* **1997**, 45, 149–154.
- (9) Langer, S. H.; Patton, J. E. *J. Phys. Chem.* **1972**, 76, 2159–2169.
- (10) Coca, J.; Medina, I.; Langer, S. H. *Liq. Cryst.* **1989**, 4, 175–180.
- (11) Coca, J.; Adrio, G.; Langer, S. H. *Chem. Eng. Sci.* **1988**, 43, 2007–2012.
- (12) Langer, S. H.; Sheehan, R. J.; Huang, J. C. *J. Phys. Chem.* **1982**, 86, 4605–4618.
- (13) Huang, J. C.; Langer, S. H.; Sheehan, R. J. *J. Phys. Chem. B* **2004**, 108, 4422–4431.
- (14) Langer, S. H.; Purnell, J. H. *J. Phys. Chem.* **1963**, 67, 263–270.
- (15) Langer, S. H.; Purnell, J. H. *J. Phys. Chem.* **1966**, 70, 904–909.
- (16) Huang, J. C. *J. Chromatog.* **1985**, 321, 458–461.
- (17) Bell, R. P. *Trans. Faraday Soc.* **1937**, 33, 496–501.
- (18) Leffler, J. E.; Grunwald, E. *Rates and Equilibrium of Organic Reactions*; Wiley: New York, 1963.
- (19) Eckert, C. A.; Hsieh, C. K.; McCabe, J. R. *AIChE J.* **1974**, 20, 20–36.
- (20) Qian, J. H.; Hopfield, J. J. *Chem. Phys.* **1996**, 105, 9292–9298.
- (21) Cooper, A.; Johnson, C. M.; Lakey, J. H.; Nöllman, M. *Biophys. Chem.* **2001**, 93, 215–230.
- (22) Sharp, K. *Protein Sci.* **2001**, 10, 661–667.
- (23) Liu, L.; Guo, Q. X. *Chem. Rev.* **2001**, 101, 673–695.
- (24) Krug, R. R.; Hunter, R. H.; Grieger, R. A. *J. Phys. Chem.* **1976**, 80, 2335–2440.
- (25) Krug, R. R.; Hunter, R. H.; Grieger, R. A. *J. Phys. Chem.* **1976**, 80, 2341–2451.
- (26) Li, J.; Carr, P. W. *J. Chromatogr. A* **1994**, 670 (1–2), 105–116.
- (27) Vailaya, A.; Horváth, C. *Ind. Eng. Chem. Res.* **1996**, 35, 2964–2981.
- (28) Vailaya, A.; Horváth, C. *J. Phys. Chem. B* **1998**, 102, 701–718.
- (29) Langer, S. H.; Sheehan, R. J. *J. Chem. Eng. Data* **1969**, 14, 248–250.
- (30) Reid, R. C.; Prausnitz, J. M.; Poling, B. E. *The Properties of Gases and Liquids*, 4th ed.; McGraw-Hill: New York, 1987.
- (31) Flory, P. J. *J. Chem. Phys.* **1942**, 10, 51–61.
- (32) Huggins, M. L. *Ann. N. Y. Acad. Sci.* **1942**, 43, 1–32.
- (33) Flory, P. J. *Principles of Polymer Chemistry*; Cornell University Press: New York, 1953.
- (34) Flory, P. J. *Discuss. Faraday Soc.* **1970**, 49, 7–29.
- (35) Guggenheim, E. D. *Trans. Faraday Soc.* **1948**, 44, 1007–1012.
- (36) Krug, R.; Hunter, W.; Grieger, R. A. *Nature* **1976**, 261, 566–567.
- (37) Sheehan, R. J. Ph.D. Thesis, Department of Chemical Engineering University of Wisconsin–Madison, 1968.
- (38) Hildebrand, J. H.; Prausnitz, J. M.; Scott, R. L. *Regulated and Related Solutions*; Van Nostrand Reinhold Co.: New York, 1970.
- (39) Langer, S. H.; Sheehan, R. J. In *Advances in Analytical Chemistry and Instrument*; Purnell, J. H., Ed.; 1968; Vol 6, pp 289–324.
- (40) Sheehan, R. J.; Langer, S. H. *Ind. Eng. Chem. Process Des. Dev.* **1971**, 10, 44–46.
- (41) Vitha, M. F.; Carr, P. W. *J. Phys. Chem. B* **2000**, 104, 5343–5349.
- (42) Flory, P. J.; Orwoll, R. A.; Vrij, A. *J. Am. Chem. Soc.* **1964**, 86, 3507–3514, 3515–3520.
- (43) Becerra, M. R.; Fernández-Sánchez, E.; Fernández-Torres, A.; Garca-Dominguez, J. A.; Santiuste, J. M. *Macromolecules* **1992**, 25, 4665–4670.
- (44) Galin, M. *Polymer* **1983**, 24, 865–870.
- (45) Humpa, O.; Uhdeová, J.; Roth, M. *Macromolecules* **1991**, 24, 2514–2517.
- (46) Pierotti, G. J.; Deal, C. H.; Derr, E. L. *J. Am. Chem. Soc.* **1956**, 78, 2989–2998.
- (47) Pierotti, G. J.; Deal, C. H.; Derr, E. L.; Porter, P. E. *Ind. Eng. Chem.* **1959**, 51, 95–102.
- (48) Demathieu, C.; Chehimi, M. M.; Lipskier, J.-F. *Sens. Actuators B* **2000**, 62, 1–7.